Formation, Crystal Structure, and Rearrangement of a Cytochrome P-450$_{cam}$ Iron–Phenyl Complex†

Reetta Raag,‡ Barbara A. Swanson,§ Thomas L. Poulos,‡,‖ and Paul R. Ortiz de Montellano*,§

Center for Advanced Research in Biotechnology of the Maryland Biotechnology Institute, University of Maryland, Shady Grove, 9600 Gudelsky Drive, Rockville, Maryland 20850, Department of Chemistry and Biochemistry, University of Maryland, College Park, Maryland 20742, and Department of Pharmaceutical Chemistry, School of Pharmacy, University of California, San Francisco, California 94143-0446

Received March 26, 1990; Revised Manuscript Received May 18, 1990

ABSTRACT: Cytochrome P-450$_{cam}$ reacts with phenyldiazene (PhN=NH), or less efficiently with phenylhydrazine, to give a catalytically inactive complex with an absorption maximum at 474 nm. The prosthetic group extracted anaerobically from the inactivated protein has the spectroscopic properties of a σ phenyl–iron complex and rearranges, on exposure to air and acid, to an approximately equal mixture of the four *N*-phenylprotoporphyrin IX regioisomers. The crystal structure of the intact protein complex, refined at 1.9-Å resolution to an *R* factor of 20%, confirms that the phenyl group is directly bonded through one of its carbons to the iron atom. The phenyl ring is tilted from the heme normal by about 10° in the opposite direction from that in which carbon monoxide tilts when bound to P-450$_{cam}$. Camphor, the natural substrate for P-450$_{cam}$, is larger than a phenyl group and hydrogen bonds to Tyr 96, the only hydrophilic residue near the active site. Electron density in the active site in addition to that contributed by the phenyl group suggests that two water molecules occupy part of the camphor binding site but are not within hydrogen-bonding distance of Tyr 96. As observed in a previous crystallographic study of inhibitor–P-450$_{cam}$ complexes [Poulos, T. L., & Howard, A. J. (1987) *Biochemistry 26*, 8165–8174], there are large changes in both the atomic positions and mobilities of the residues in the proposed substrate access channel region of the protein. Furthermore, both the distal and proximal helix regions appear to be perturbed in the σ-bonded phenyl–iron complex. Unambiguous characterization of the phenyldiazene complex of cytochrome P-450$_{cam}$ makes possible the use of such complexes to probe the active site topologies of membrane-bound cytochrome P-450 enzymes.

The cytochrome P-450 monooxygenases are hemoproteins that are involved in many physiologically important processes, including the biosynthesis of steroids, the metabolism of drugs and other xenobiotics, and the biological activation of procarcinogens. Their pivotal function in biosynthetic, catabolic, and toxicological processes makes their inhibition of considerable pharmacological and toxicological importance. Cytochrome P-450 enzymes can be inhibited by competitive displacement of substrates from their binding site, chemical modification of the protein or the porphyrin, or either coordination or full covalent binding to the porphyrin iron atom (Ortiz de Montellano & Reich, 1986). Reversible inhibition by agents that either compete for occupancy of the active site or coordinate to the iron is fairly well understood as the result of extensive work in the area, including determination of the crystal structures of the complexes formed by cytochrome P-450$_{cam}$[1] with metyrapone and several substituted imidazoles (Poulos & Howard, 1987). These crystallographic studies have provided structural explanations for the differences in the spectroscopic properties and binding constants of the phenylimidazole regioisomers (Poulos & Howard, 1987).

Much less definitive structural information is available on complexes in which a carbon–iron bond is thought to result from catalytic processing of the inhibitors within the active site of the cytochrome P-450 enzyme that is inactivated. The halocarbons, alkyl- and arylhydrazines, (methylenedioxy)benzenes, and diazo compounds are among the agents thought to act by this mechanism (Ortiz de Montellano & Reich, 1986). Differences in the spectroscopic properties of the resulting complexes, however, suggest the formation of more than one type of carbon–iron bond. Thus, the complexes formed by microsomal cytochrome P-450 with polyhalomethanes (e.g., CCl_4, CCl_3F, $CHCl_3$) have absorption maxima at 452–465 nm (Uehleke et al., 1973; Cox et al., 1976; Wolf et al., 1977) whereas those formed with alkyldiazenes (CH_3CH_2N=NH, $PhCH_2N$=NH) and some halogenated hydrocarbons (e.g., $CF_3CHClBr$, $PhCH_2Br$) have maxima at 470–480 nm (Ruf et al., 1984; Mansuy & Fontecave, 1983; Battioni et al., 1983). The complex formed in the reaction of microsomal cytochrome P-450 with phenylhydrazine also has a maximum at 480 nm (Jonen et al., 1982; Delaforge et al., 1986), but the complex between microsomal cytochrome P-450 and 1,2-(methylenedioxy)benzene exhibits bands at 427 and 455 nm in microsomes from phenobarbital-induced rats but a single band at 456 nm in microsomes from β-naphthoflavone-induced rats (Elcombe et al., 1975; Marcus et al., 1985).

Substantial uncertainty exists concerning the structure of the bound residue and the nature of the carbon–iron bond in the cytochrome P-450 complexes despite the clues provided

† This work was supported by Grants GM 25515 (P.R.O.M.) and GM 33688 (T.L.P.) from the National Institutes of Health.

* Address correspondence to this author.
‡ University of Maryland, Shady Grove.
§ University of California, San Francisco.
‖ University of Maryland, College Park.

[1] Abbreviations: cytochrome P-450$_{cam}$, common name for the enzyme formally classified as cytochrome P450CIA1 (Nebert et al., 1987); F_o, observed structure factors; F_c, calculated structure factors; NMR, nuclear magnetic resonance spectroscopy; HPLC, high-pressure liquid chromatography; heme, iron protoporphyrin IX regardless of the oxidation and ligation states.

0006-2960/90/0429-8119$02.50/0

by well-characterized metalloporphyrin models. X-ray crystallography has documented the formation of several carbon–iron complexes: (a) a carbene–iron complex in the reaction of iron(II) tetraphenylporphyrin with CCl_4 (Mansuy et al., 1978, 1979), (b) a complex with a carbon bridging the iron and a pyrrole nitrogen in the reaction of the same metalloporphyrin with Ar_2CHCCl_3 (Chevrier et al., 1981; Olmstead et al., 1982), and (c) a complex with a phenyl group σ-bonded to the iron atom in the reaction with $AgBPh_4$ (Doppelt, 1984). In the present context, the most relevant crystallographic model is that of the complex formed by the reaction of myoglobin with phenylhydrazine, which shows that the phenyl group is directly attached to the iron by a σ-bond (Ringe et al., 1984). This result clearly suggests a similar structure for the complex formed by reaction of cytochrome P-450 with phenyldiazene, but the differences in the *trans*-iron ligand (imidazole vs thiolate) and the polarity and functionality of the active sites of myoglobin and cytochrome P-450 require caution in extrapolating the structure of the one complex to the other.

Metalloporphyrin alkyl–, aryl–, and vinyl–iron complexes rearrange to *N*-alkyl–, *N*-aryl–, and *N*-vinylporphyrin adducts, respectively, under acidic, oxidative conditions (Augusto et al., 1982; Mansuy et al., 1982a; Ortiz de Montellano et al., 1982; Ortiz de Montellano & Reich, 1986). The iron–phenyl complex of *meso*-tetraphenylporphyrin (Kunze & Ortiz de Montellano, 1983) is thus converted by oxygen or other oxidizing agents to *N*-phenyl-*meso*-tetraphenylporphyrin. Electrochemical and NMR studies of the *meso*-tetraarylporphyrin complexes show that oxidation of the iron to the Fe^{4+} state triggers the phenyl shift because migration to the nitrogen reduces the hypervalent iron to the energetically more favored ferrous state (Lançon et al., 1984; Balch & Renner, 1986). The same process occurs when the protoporphyrin IX iron–phenyl complex is extracted from hemoglobin under aerobic, acidic conditions. *N*-Phenylprotoporphyrin IX is isolated under those conditions whereas the heme group is recovered intact if the complex is isolated without exposure to oxygen (Augusto et al., 1982; Mansuy et al., 1982b). The end products of the reaction of cytochrome P-450 with phenylhydrazine or phenyldiazene were not determined in earlier studies (Jonen et al., 1982; Delaforge et al., 1986).

The crystallographic studies of both the phenylhydrazine–myoglobin (Ringe et al., 1984) and nitrogenous inhibitor–P-450_{cam} (Poulos & Howard, 1987) complexes show that inhibitor binding causes specific regions of the proteins, previously suggested to be substrate or ligand access channels, to undergo large changes either in mean-square displacements or in mobility (atomic temperature factors) relative to the uncomplexed structures. In the myoglobin complex (Ringe et al., 1984), side chains actually move away to generate an open channel to the ligand-binding pocket that is solvent inaccessible in the water-ligated metmyoglobin state. The cytochrome P-450_{cam} inhibitors, besides causing enhanced mobility of residues in the proposed substrate access channel region, also cause large structural changes in the distal helix region (Poulos & Howard, 1987).

Here we report the formation, chemical characterization, and X-ray crystal structure of the complex formed in the reaction of phenyldiazene with cytochrome P-450_{cam}, the camphor hydroxylase from *Pseudomonas putida* (Wagner & Gunsalus, 1982; Sligar & Murray, 1986; Gunsalus & Sligar, 1978; Dawson & Sono, 1987). The results definitively establish the structure of the first carbon–iron complex of cytochrome P-450 other than that with carbon monoxide and, by exclusion, facilitate clarification of the structures of other such complexes. They also make possible use of the iron–phenyl complex to probe the active site topologies, and the absolute orientation of the heme group, in membrane-bound cytochrome P-450 enzymes.

Materials and Methods

Chemical Characterization of the Phenyldiazene–Cytochrome P-450_{cam} Complex. Cytochrome P-450_{cam}, purified by a modification of the procedure of Gunsalus and Wagner (1978b), was passed through a small Sephadex G-15 column with 50 mM potassium phosphate buffer (pH 7.0) to remove the camphor ligand. To 5–6 nmol of this cytochrome P-450_{cam} in 0.6–1.0 mL of buffer was added sufficient phenyldiazene to completely form the complex within 15 min. Phenyldiazene was generated by adding 2.5 μL of methyl phenyldiazenecarboxylate azo ester (Research Organics, Inc.) to 200 μL of 1 M NaOH (Kosower & Huang, 1965). Approximately 2 μL of this solution was generally required to completely convert cytochrome P-450_{cam} to the complex. Complex formation was monitored by the increase in the absorption maximum at 474 nm and the associated decrease in the Soret maximum at 416 nm.

The complex prepared above was made anaerobic by sweeping the protein solution with a stream of argon for 1 h. Sufficient (usually 5–10 μL) glacial acetic acid then was added to bring the solution to pH 4.0. The reddish heme complex was extracted with argon-saturated 2-butanone containing 0.025% (w/v) butylated hydroxytoluene (BHT) (Kunze & Ortiz de Montellano, 1983). The extracts were placed in an argon-flushed flask, and a volume of acetonitrile equal to that of the combined extracts (generally about 300 μL) and 100 μL of 5% (v/v) sulfuric acid in water were added. The resulting solution was made aerobic by opening the flask and bubbling with air for several minutes. Within an hour the solution became green. It then was concentrated on a rotary evaporator, and the concentrate was extracted with methylene chloride.

The residue obtained after evaporation of the methylene chloride was dissolved in 50 μL of solvent A (see below) and was analyzed by reverse-phase HPLC on a Hewlett Packard 1090 liquid chromatography system fitted with a 25 × 4.6 cm column packed with Partisil ODS-3 (5 μm). The column was eluted isocratically for 30 min with 80% solvent A (6:4:1 methanol/water/glacial acetic acid) and 20% solvent B (10:1 methanol/glacial acetic acid). A flow rate of 1 mL/min was maintained, and the column was monitored at 410 nm with a diode array detector. The column was washed with 100% solvent B at the end of each run. Authentic samples of the four *N*-phenylprotoporphyrin IX isomers were obtained by analogous extraction of the prosthetic group of phenylhydrazine-treated horse myoglobin (Augusto et al., 1982).

Preparation of Cytochrome P-450_{cam} Complex for X-ray Studies. Cytochrome P-450_{cam} was crystallized as described earlier (Poulos et al., 1982). The artificial mother liquor used for soaking crystals consisted of 40% ammonium sulfate, 0.25 M KCl, and 0.05 M potassium phosphate, pH 7.0. The cytochrome P-450-inhibitor complex was prepared essentially as described above. Phenyldiazene was freshly prepared immediately before use by base hydrolysis of phenyldiazenecarboxylate azo ester. A 5-μL sample of the ester was added to 0.4 mL of argon-saturated 1.0 M KOH, and the solution was bubbled with argon for about 40 min. A 25-μL aliquot of this solution was added to the argon-saturated mother liquor containing cytochrome P-450_{cam} crystals. After soaking for 5 h at room temperature, the crystals were mounted in an

Table I: Summary of Data Collection

maximum resolution (Å)	1.87
total observations	128 716
R_{sym}[a]	0.074
% data collected to	
3.40 Å	100
2.70 Å	100
2.36 Å	100
2.14 Å	97
1.99 Å	55
1.87 Å	37
$I/\sigma(I)$	
2.36 Å	3.39
2.14 Å	1.76
1.99 Å	1.17
1.87 Å	0.55

[a] $R_{sym} = \sum|I_i - \langle I_i\rangle|/\sum I_i$, where I_i = intensity of the ith observation and $\langle I_i\rangle$ = mean intensity.

Table II: Summary of Crystallographic Refinement

resolution range (Å)	10.0–1.9
reflections measured	27 666
reflections used, $I > 2\sigma(I)$	20 765
R factor[a]	0.199
rms deviation of bond distances (Å)	0.020
rms deviation of bond angles (Å)	0.031
rms deviation of dihedral angles (Å)	0.036

[a] $R = \sum|F_o - F_c|/\sum F_o$.

X-ray capillary in preparation for data collection.

X-ray diffraction data were collected from a single crystal of the inhibitor–P-450$_{cam}$ complex by use of a Siemens area detector and a Rigaku rotating anode. Although nominally the diffraction data extend to approximately 1.9 Å for the phenyl inhibitor–P-450$_{cam}$ complex, they are relatively complete only to about 2.1 Å as can be seen from the summary of data collection statistics presented in Table I.

Crystallographic refinement was carried out by using the restrained parameters–least-squares package of programs (Hendrickson & Konnert, 1980) and is summarized in Table II. Comparison of both coordinate and temperature factor shifts was carried out as described in an earlier study (Poulos & Howard, 1987). Initial $F_o - F_c$[1] and $2F_o - F_c$ difference Fourier maps were based on structure factor calculations using coordinates from the 1.63-Å refined camphor–P-450$_{cam}$ structure (Poulos et al., 1987) and diffraction data obtained from the inhibitor–P-450$_{cam}$ complex. Camphor coordinates were not included in the structure factor calculations. A bond between the inhibitor and the heme iron atom was clearly evident in the electron density maps. A model phenyl ring, treated as a group separate from the heme throughout refinement, was positioned into the initial $F_o - F_c$ and $2F_o - F_c$ maps and refined together with the protein. Positioning of the phenyl ring was relatively straightforward in that the electron density bound to the heme iron atom was quite flat, indicating that the inhibitor binds in a single major orientation and does not rotate freely about the bond between the phenyl ring and iron atom. Additional density was also present near Tyr 96, a residue that hydrogen bonds to the natural substrate, camphor. This extra density was tentatively assumed to be two water molecules hydrogen bonding to Tyr 96 and taking up the room left in the active site by the binding of the smaller inhibitor molecule. However, active site solvent was not included in the model until about halfway through the refinement when it was clear that the inhibitor alone could not account for all of the active site electron density.

The structure was judged to have refined sufficiently once $F_o - F_c$ maps showed little or no interpretable density when contoured at $\pm 3\sigma$ (σ is the standard deviation of the difference electron density calculated over the entire asymmetric unit). The refined model was subsequently subjected to refinement without bond, angle, or nonbonded contact distance restraints to better estimate the iron–inhibitor distance.

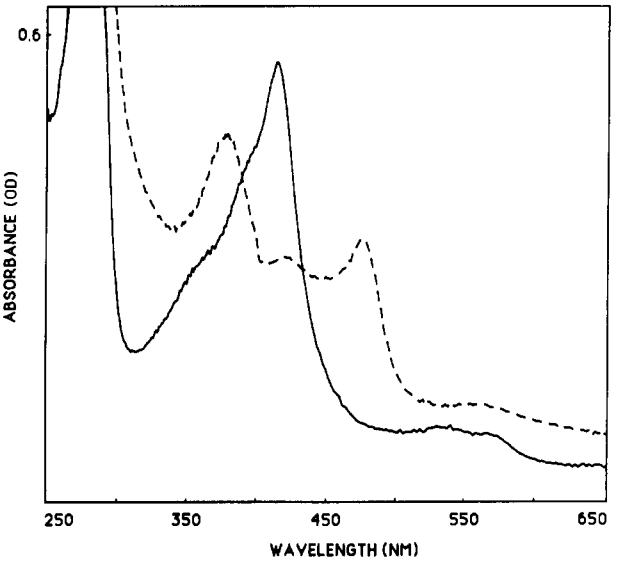

FIGURE 1: Absorption spectra at pH 7.0 of cytochrome P-450$_{cam}$ (solid line) and cytochrome P-450$_{cam}$ after reaction with phenyldiazene (dashed line) as described under Materials and Methods.

Results and Discussion

Aerobic reaction of phenyldiazene with cytochrome P-450$_{cam}$ results in a rapid decrease in the Soret band at 416 nm and the appearance of a new maximum at 474 nm (Figure 1). The same but weaker spectrum is obtained if phenylhydrazine is used rather than phenyldiazene, its oxidation product. The phenyldiazene complex, as shown by monitoring its absorbance at 474 nm, is stable in the absence of protein denaturation to oxidants such as $K_3Fe(CN)_6$, $Co^{III}(NH_3)_6Cl_3$, H_2O_2, or oxygen. The long-wavelength band is lost over several hours, however, if the cytochrome P-450$_{cam}$ complex is incubated with putidaredoxin and $K_3Fe(CN)_6$. No N-phenyl adducts are detected, however, when the prosthetic group is removed from the resulting protein and is analyzed by HPLC (see below). The reaction of phenyldiazene with cytochrome P-450$_{cam}$ thus results in the formation of a complex with an absorbance maximum similar to, but not identical with, that of the rat liver microsomal cytochrome P-450 complex (Jonen et al., 1982). The microsomal complex, however, unlike that formed with P-450$_{cam}$, is sensitive to oxidizing agents (Jonen et al., 1982).

Anaerobic extraction of the prosthetic group of the phenyldiazene–P-450$_{cam}$ complex followed by exposure to air and strong acid, conditions similar to those used earlier to characterize the complex formed with hemoglobin (Augusto et al., 1982), provides the four isomers of N-phenylprotoporphyrin IX in substantial yield (Figure 2). The spectrum of the anaerobically extracted complex prior to exposure to air and acid is identical with that obtained when the prosthetic group of myoglobin is similarly extracted (Figure 3). A σ phenyl–iron complex was shown earlier to be extracted anaerobically from phenylhydrazine-modified myoglobin (Kunze & Ortiz de Montellano, 1983; Ringe et al., 1984) and the phenyl in the isolated iron protoporphyrin IX complex shown to migrate to the pyrrole nitrogens when exposed to air and acid (Augusto et al., 1982). The fact that the species isolated from cytochrome P-450$_{cam}$ has the same spectrum as the complex isolated from myoglobin and, like it, rearranges to the N-

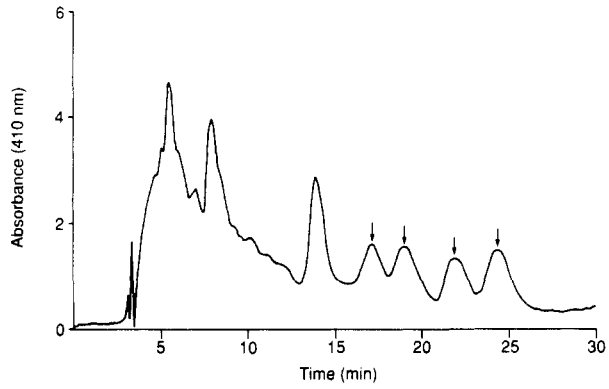

FIGURE 2: HPLC of the *N*-phenylprotoporphyrin IX isomers derived from phenyldiazene-treated cytochrome P-450$_{cam}$. The isomers were run isocratically on a 5-μm reverse-phase Partisil ODS-3 column eluted with 80% solvent A (6:4:1 MeOH/H_2O/acetic acid) and 20% solvent B (10:1 MeOH/acetic acid) at a flow rate of 1 mL/min. The eluent was monitored at 410 nm. The four *N*-phenylprotoporphyrin IX isomers, indicated by arrows, have elution times of 17.1, 19.1, 22.0, and 24.5 min. The peak areas account, respectively, for 25, 27, 21, and 27% of the total *N*-phenyl adduct. The small differences in the proportions of these peaks may not be significant because peak overlap makes integration imprecise. The identities of the compounds have been confirmed by spectroscopic and chromatographic comparisons with authentic *N*-phenylprotoporphyrin IX isomers.

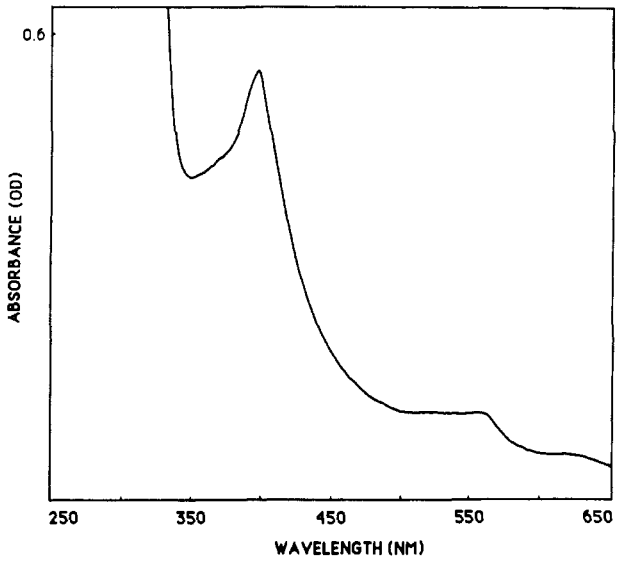

FIGURE 3: Absorption spectrum of the prosthetic heme complex extracted anaerobically from cytochrome P-450$_{cam}$. Exactly the same spectrum is obtained when the iron–phenyl complex is extracted from phenylhydrazine-treated myoglobin.

phenylprotoporphyrin IX isomers under aerobic, acidic conditions indicates that it also is the σ phenyl–iron complex of protoporphyrin IX.

It was not possible in earlier studies to separate the four regioisomers of *N*-phenylprotoporphyrin IX despite efforts to do so (Augusto et al., 1982; Ortiz de Montellano & Kerr, 1983). The HPLC system used to separate *N*-alkylprotoporphyrin IX isomers does not separate the *N*-phenyl isomers (Kunze & Ortiz de Montellano, 1981). A protocol has recently been developed, however, that results in clean separation of the four regioisomers of *N*-phenylprotoporphyrin IX (B. A. Swanson, G. D. DePillis, and P. R. Ortiz de Montellano, unpublished results). Analysis of the *N*-phenylprotoporphyrin IX formed by aerobic shift of the phenyl group of the iron–phenyl complex extracted anaerobically from phenyldiazene-inactivated cytochrome P-450 shows that the four regioisomers are formed in essentially equal amounts. This establishes that there is no significant inherent preference for the phenyl group to shift to any of the four pyrrole nitrogens. The four regioisomers are not formed in equal amounts when the phenyl group of the analogous mammalian cytochrome P-450 complexes is induced to migrate within the intact protein by the action of oxidizing agents (B. A. Swanson and P. R. Ortiz de Montellano, unpublished results). The resistance of the cytochrome P-450$_{cam}$ complex to oxidizing agents has prevented a study of the phenyl group migration within its active site.

In order to fully define the structure of the intact cytochrome P-450$_{cam}$ complex and its interactions with the protein structure, the crystal structure of the complex has been determined. The initial $F_o - F_c$ difference Fourier map for the ferric phenyl inhibitor complex of P-450$_{cam}$ is shown in Figure 4. The final refined $2F_o - F_c$ map is shown in Figure 5. The Fe–phenyl inhibitor distance refined to 2.07 Å in the presence, and 1.65 Å in the absence, of van der Waals restraints. The phenyl inhibitor is bound at an angle of about 10° to the heme normal (Figure 6). It is interesting that this is about the same angle at which carbon monoxide (CO) was found to bind to ferrous camphor-bound P-450$_{cam}$ (Raag & Poulos, 1989b). However, the tilt of the phenyl inhibitor is in the opposite direction from that of carbon monoxide. In our earlier work we attributed the tilting of the distal axial CO ligand to van der Waals clashes primarily with camphor (Raag & Poulos, 1989b). In the inhibitor–P-450$_{cam}$ structure, camphor is not present but its approximate position is occupied by two water molecules which, however, are too far away to be hydrogen bonded to Tyr 96. Although the phenyl inhibitor and CO both bind to the heme iron atom, CO is able to fit into a groove in the distal helix whereas the phenyl inhibitor binds face-on toward this helix and is apparently forced by the resulting van der Waals contacts to bend toward the waters near Tyr 96. These two waters also do not occupy as much room as does the camphor molecule, allowing the inhibitor to tilt to a position that CO could not occupy in the presence of camphor. It does not appear to be sterically possible for the phenyl inhibitor to rotate 90° about the carbon–iron bond in order to fit edge-on into the distal helix groove that CO fits into (Figure 7). Moreover, there is potentially an attractive electrostatic component to CO tilting toward the distal helix groove which is not present with the hydrophobic phenyl inhibitor. The groove in the distal helix which CO fits into is formed by a hydrogen bond between the side-chain hydroxyl group of Thr 252 and the backbone carbonyl of Gly 248 of the distal helix (Poulos et al., 1987) and has been proposed to be a conserved feature of all P-450s, bacterial as well as eukaryotic, on the basis of sequence alignments (Poulos et al., 1987; Nelson & Strobel, 1988). The observation that CO fits into the groove further suggests that the catalytically productive O_2–camphor–P-450$_{cam}$ complex will have a similar structure (Raag & Poulos, 1989b).

A comparison of refined camphor–P-450$_{cam}$ and phenyl–P-450$_{cam}$ coordinates indicates that there are relatively large shifts in the positions of protein atoms between the camphor- and phenyl-bound forms (Figure 6). The largest changes are found in the distal and proximal helix regions and in the residues surrounding the proposed access channel (Poulos et al., 1987; Poulos & Howard, 1987). The largest increases in individual atomic temperature factors and hence, presumably, in atomic mobilities were also found to be in the substrate access channel region and the loop containing Tyr 96, the residue which forms a 2.7-Å hydrogen bond with camphor. As mentioned previously, two water molecules occupy the approximate position of camphor in the presence of the phenyl inhibitor, but these

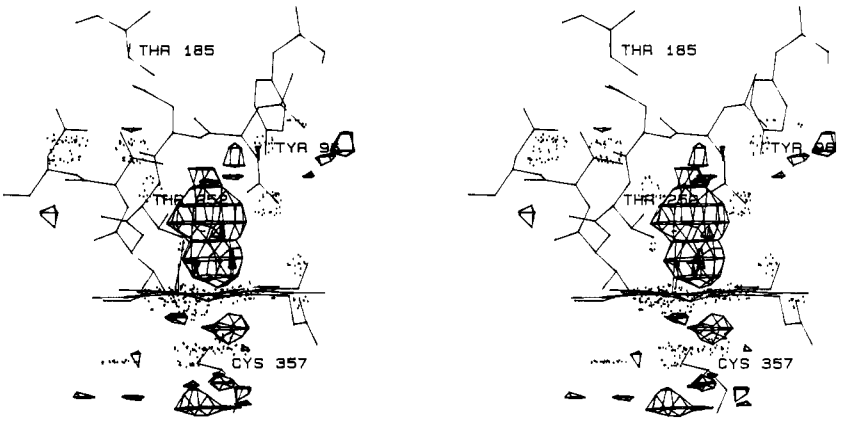

FIGURE 4: Stereoscopic view of the initial $F_o - F_c$ electron density map for the ferric inhibitor–P-450$_{cam}$ complex, contoured at $\pm 3\sigma$ with the negative contours shown as dashed lines, and superimposed on the model for the camphor–P-450$_{cam}$ complex (camphor coordinates have been removed for clarity). Note that this view of the active site is about a 90° rotation around a vertical axis away from the "usual" view of Figure 5 and shows the difference electron density representing the phenyl inhibitor essentially face on. The distribution of positive and negative difference electron density (as well as the bilobal shape of the inhibitor density) in this initial map suggests that, with respect to the ferric camphor-bound P-450$_{cam}$ complex, binding of a phenyl radical results in movement of the proximal cysteine ligand toward the heme and movement of the iron atom into the heme plane. These changes were indeed observed as a result of refinement and are shown in Figure 6.

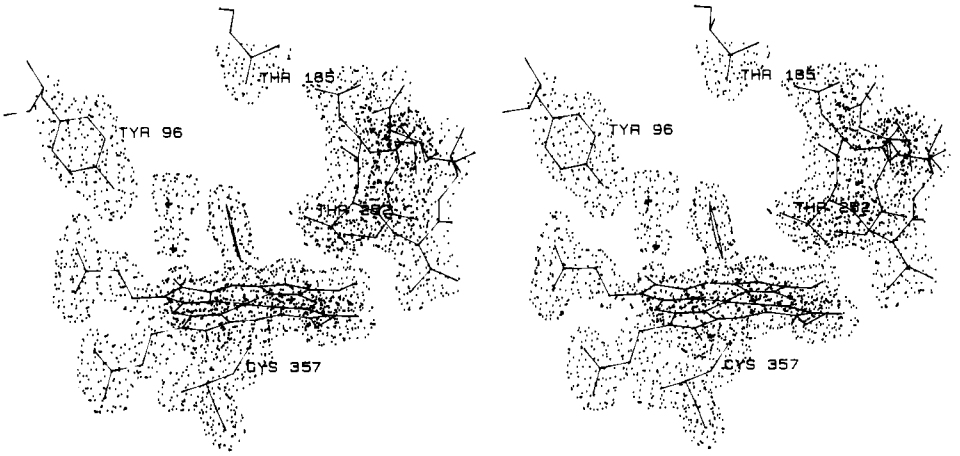

FIGURE 5: Stereoscopic view of the final $2F_o - F_c$ electron density map for the ferric inhibitor–P-450$_{cam}$ complex, contoured at $\pm 1\sigma$, superimposed on the final refined coordinates for this complex. Note the residual electron density which has been interpreted as two water molecules between Tyr 96 and the phenyl inhibitor. Coordinates for the inhibitor and for both active site water molecules were omitted from the phase calculation for the map shown.

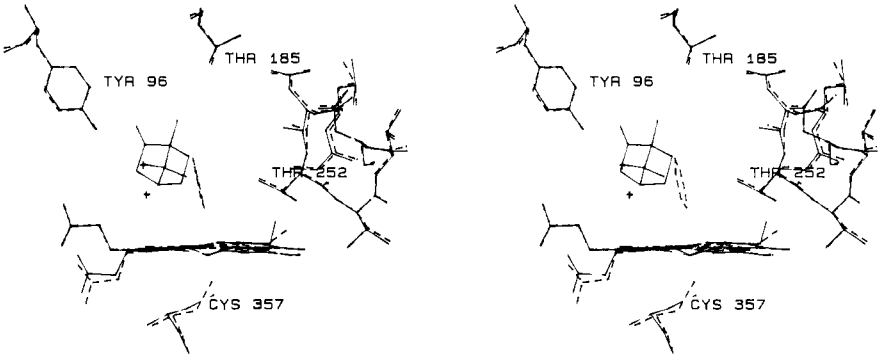

FIGURE 6: Stereoscopic model of the refined inhibitor–P-450$_{cam}$ complex superimposed on the refined model of the camphor–P-450$_{cam}$ complex. The camphor–P-450$_{cam}$ complex is shown with solid bonds and the inhibitor–P-450$_{cam}$ complex with dashed bonds. Crosses represent the active site water molecules present in the inhibitor–P-450$_{cam}$ complex.

water molecules are 4.8 and 5.0 Å from the side-chain hydroxyl group of Tyr 96, too far to dampen the motion of this substrate-contacting loop by hydrogen bonding.

The average temperature factors for the camphor and phenyl atoms are 16.2 Å^2 and 19.8 Å^2, respectively. These values are not very different, especially since the rms difference of all protein and heme atom temperature factors between the camphor–P-450$_{cam}$ and the phenyl–P-450$_{cam}$ structures is 2.7 Å^2. Although camphor is larger than a phenyl ring, both of these compounds are rather firmly held in position in the active site of P-450$_{cam}$, the former by a hydrogen bond and the latter by the iron–carbon σ-bond.

It should be noted that $F_o - F_c$ maps for the phenyl–P-450$_{cam}$ complex are considerably "noisier", containing more uninterpretable difference electron density, than the corresponding maps for a variety of substrate–P-450$_{cam}$ complexes (Raag &

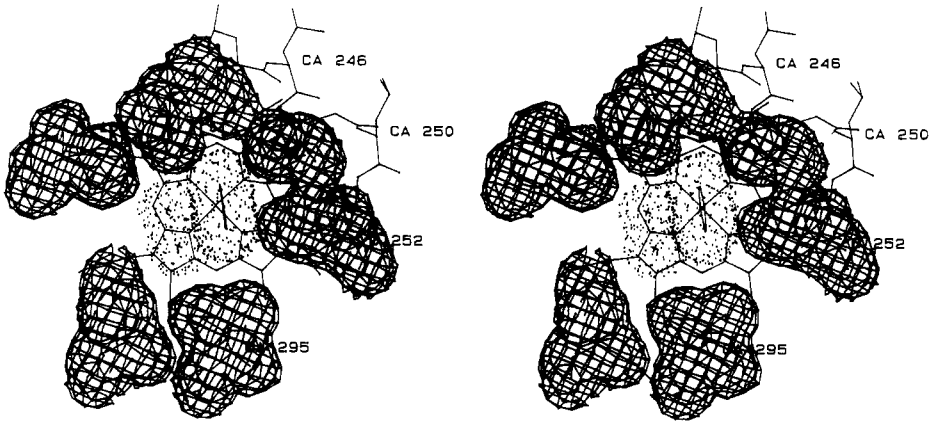

FIGURE 7: View of the phenyl–iron complex from above showing the van der Waals radii of the residues in the immediate vicinity of the phenyl–iron complex (dark contours). The van der Waals surface of the phenyl group and the two water molecules is shown as a dotted surface. The crosses represent the active site water molecules.

Poulos, 1989a,b). A P-450$_{cam}$ crystal was soaked in phenyldiazene for 7 days to determine whether soak time affected the "extra" electron density observed in the active site after the 5-h soak. However, the data quality from this second crystal was statistically quite poor and the resultant electron density map too disconnected and ambiguous to interpret reliably. We believe this may be due to increased nonspecific binding of the phenyl radical to P-450$_{cam}$ over the prolonged soaking period. We did not find large lobes of positive electron density on the surface of P-450$_{cam}$ soaked for a few hours in phenyldiazene, a result that does not rule out nonspecific binding of phenyl radicals.

An additional experiment was motivated by the suggestion of Itano and Mannen (1976) that two processes occur simultaneously in the reaction of phenyldiazene with ferrihemoglobin, reduction of ferrihemoglobin to ferrohemoglobin and production of ferrihemochrome species later identified as phenyl–iron complexes. They also reported that ferrohemoglobin does not form a ferrohemochrome with phenyldiazene. These results suggest the possibility that a portion of the ferrihemoglobin molecules might react with phenyl radicals produced by the oxidation of phenyldiazene by other ferrihemoglobin molecules which thus become ferrohemoglobins not susceptible to reaction with phenyl radicals (Itano & Mannen, 1976).

To test whether our electron density maps represented an average of a population in which a portion of the molecules in the crystalline lattice were ferric and inhibitor–P-450$_{cam}$ complexes and the remainder were ferrous, pentacoordinate P-450$_{cam}$ molecules, we varied the occupancy of the phenyl inhibitor and of all solvent molecules in our model. The results of this experiment cannot be considered conclusive, however, because although P-450$_{cam}$ was derivatized with phenyldiazene in the presence of argon, oxygen was not rigorously excluded. Thus, if the refined occupancy of the inhibitor were less than 1.0 (fully occupied), it could not be assumed that a portion of the cytochrome P-450 molecules in the crystal oxidized phenyldiazene and remained underivatized. Instead, our soak time of only a few hours may have been insufficient to allow the inhibitor to react with all P-450 molecules in the crystal. On the other hand, if the inhibitor occupancy remained at unity, this result would not demonstrate that both ferrous and ferric P-450$_{cam}$ are subject to attack by the phenyl radical. Again, phenyldiazene may have been oxidized by oxygen and not by the heme enzyme. Nevertheless, it is interesting to know the occupancies of nonprotein groups in the active site because occupancies near unity would suggest that a model consisting of two water molecules and a phenyl ring is adequate to describe the active site electron density.

The result of allowing the occupancies of the phenyl inhibitor atoms to refine was that the occupancy of the carbon atom nearest (and presumably bound to) the heme iron atom remained at 1.0 whereas the occupancies of all the other carbons of the phenyl group refined to values between 0.74 and 0.97, with no obvious correlation between distance to the iron atom and occupancy. Since the average occupancy for the phenyl inhibitor is 0.88, and 0.77 and 0.89 for the two active site waters, these groups probably represent reasonably well the actual inhibited P-450$_{cam}$ active site. The two water molecules have relatively high temperature factors (atomic mobilities) of 22.4 Å^2 and 28.8 Å^2, indicating that they probably do not occupy well-defined locations in the active site. An ill-defined cluster of active site waters also characterized the camphor-free ferric P-450$_{cam}$ structure (Poulos et al., 1986). Furthermore, none of these water molecules was sufficiently close to Tyr 96 to hydrogen bond with it, just as neither of the active site water molecules in the presence of the phenyl inhibitor is close enough to hydrogen bond with Tyr 96.

Both the asymmetric shape of the phenyl ring electron density and the presence of additional electron density which we have interpreted as solvent could indicate that the active sites of the enzyme molecules in the crystal are heterogeneously occupied. Although unlikely for molecules in presumably identical environments, the fact that aryldiazenes can give rise to a number of oxidation products (Kosower, 1971) leaves open the possibility that different molecules in the crystal lattice have different phenyldiazene-derived species bound to their hemes. For instance, the additional electron density which we take to be solvent molecules in the active site could actually represent part of a phenyldiazenecarboxylate moiety at low occupancy. The fact that the electron density is not continuous between the "water" molecules and the phenyl group renders the modeling of larger phenyldiazene oxidation products in the active site both very difficult and quite subjective and has therefore not been attempted. In light of the nearly full occupancies of the phenyl moiety and active site water molecules, alternative diazene decomposition products, if present, are bound to only a small fraction of the P-450$_{cam}$ molecules in the crystalline lattice.

Unambiguous identification of the 474-nm species formed with phenyldiazene as the σ-bonded phenyl–iron complex is a first step toward definitive structural characterization of the various classes of hemoprotein complexes proposed to involve carbon–iron bonds. There is now little doubt that the previously reported complex of phenyldiazene with microsomal cytochrome P-450 is also a phenyl–iron complex even though

it is much more sensitive to oxidizing agents than the cytochrome P-450$_{cam}$ complex (Jonen et al., 1982). The present data also strongly support the hypothesis that the unstable complexes with bands at 478 and 486 nm observed in the reactions of microsomal cytochrome P-450 with benzyl bromide (Mansuy & Fontecave, 1983) and ethyldiazene (Battioni et al., 1983) are due, respectively, to the benzyl–iron and ethyl–iron complexes. Conversely, the present results argue that the halocarbon complexes with spectroscopic maxima in the 450–465-nm range are held together by something other than a simple carbon–iron σ-bond. The carbon–iron link in these complexes is therefore probably either a carbene–iron bond or one in which a carbon bridges the iron and a pyrrole nitrogen.

Unambiguous identification of the phenyl–iron complex formed between cytochrome P-450$_{cam}$ and phenyldiazene, and therefore of the corresponding mammalian enzyme complexes, makes the susceptibility of the mammalian complexes to oxidative phenyl migration within the intact protein a useful probe of their active sites. The pyrrole ring regiospecificity of the phenyl shift should unmask the protein topology in the immediate vicinity of the heme group. In addition, the absolute stereochemistry of the resulting *N*-phenyl adducts should define the absolute orientation of the heme group in the protein. The results of such studies will be reported in due course.

Acknowledgments

We thank Ms. Julie Fruetel for providing the purified cytochrome P-450$_{cam}$ used in chemical characterization of the phenyldiazene complex.

Registry No. P-450, 9035-51-2; PhN=NH, 931-55-5; methyl phenyldiazenecarboxylate azo ester, 2207-96-7; water, 7732-18-5.

References

Augusto, O., Kunze, K. L., & Ortiz de Montellano, P. R. (1982) *J. Biol. Chem. 257*, 6231–6241.

Balch, A. L., & Renner, M. W. (1986) *J. Am. Chem. Soc. 108*, 2603–2608.

Battioni, P., Mahy, J.-P., Delaforge, M., & Mansuy, D. (1983) *Eur. J. Biochem. 134*, 241–248.

Chevrier, B., Weiss, R., Lange, M., Chottard, J.-C., & Mansuy, D. (1981) *J. Am. Chem. Soc. 103*, 2899–2901.

Cox, P. J., King, L. J., & Parke, D. V. (1976) *Xenobiotica 6*, 363–375.

Dawson, J. H., & Sono, M. (1987) *Chem. Rev. 87*, 1255–1276.

Delaforge, M., Battioni, P., Mahy, J. P., & Mansuy, D. (1986) *Chem.-Biol. Interact. 60*, 101–114.

Doppelt, P. (1984) *Inorg. Chem. 23*, 4009–4011.

Elcombe, C. R., Bridges, J. W., Gray, T. J. B., Nimmo-Smith, R. H., & Netter, K. J. (1975) *Biochem. Pharmacol. 24*, 1427–1433.

Gunsalus, I. C., & Sligar, S. G. (1978a) *Adv. Enzymol. Relat. Areas Mol. Biol. 47*, 1–44.

Gunsalus, I. C., & Wagner, G. C. (1978b) in *Methods in Enzymology*, Vol. 52, Part C, pp 166–188, Academic Press, New York.

Hendrickson, W. A., & Konnert, J. H. (1980) in *Computing in Crystallography* (Diamond, R., Ramaseshan, S., & Venkatesan, K., Eds.) pp 1301–1323, Indian Institute of Science, Bangalore.

Huang, P.-K., & Kosower, E. M. (1968) *J. Am. Chem. Soc. 90*, 2362–2367.

Itano, H. A., & Mannen, S. A. (1976) *Biochim. Biophys. Acta 421*, 87–96.

Jonen, H. G., Werringloer, J., Prough, R. A., & Estabrook, R. W. (1982) *J. Biol. Chem. 257*, 4404–4411.

Kosower, E. M. (1971) *Acc. Chem. Res. 4*, 193–198.

Kosower, E. M., & Huang, P.-K. C. (1965) *J. Am. Chem. Soc. 87*, 4645–4646.

Kunze, K. L., & Ortiz de Montellano, P. R. (1981) *J. Chem. Soc. 103*, 4225–4230.

Kunze, K. L., & Ortiz de Montellano, P. R. (1983) *J. Am. Chem. Soc. 105*, 1380–1381.

Lançon, D., Cocolios, P., Guilard, R., & Kadish, K. M. (1984) *J. Am. Chem. Soc. 106*, 4472–4478.

Mansuy, D., & Fontecave, M. (1983) *Biochem. Pharmacol. 12*, 1871–1879.

Mansuy, D., Lange, M., Chottard, J.-C., Bartoli, J. F., Chevrier, B., & Weiss, R. (1978) *Angew. Chem., Int. Ed. Engl. 17*, 781.

Mansuy, D., Battioni, J.-P., Chottard, J.-C., & Ullrich, V. (1979) *J. Am. Chem. Soc. 101*, 3971–3973.

Mansuy, D., Battioni, J.-P., Dupre, D., Sartori, E., & Chottard, G. (1982a) *J. Am. Chem. Soc. 104*, 6159–6161.

Mansuy, D., Battioni, P., Mahy, J.-P., & Gillet, G. (1982b) *Biochem. Biophys. Res. Commun. 106*, 30–36.

Marcus, C. B., Murray, M., & Wilkinson, C. F. (1985) *Xenobiotica 15*, 351–362.

Nebert, D. W., Adesnik, M., Coon, M. J., Estabrook, R. W., Gonzalez, F. J., Guengerich, F. P., Gunsalus, I. C., Johnson, E. F., Kemper, B., Levin, W., Phillips, I. R., Sato, R., & Waterman, M. R. (1987) *DNA 6*, 1–11.

Nelson, D. R., & Strobel, H. W. (1988) *J. Biol. Chem. 263*, 6038–6050.

Olmstead, M. M., Cheng, R.-J., & Balch, A. L. (1982) *Inorg. Chem. 21*, 4143–4148.

Ortiz de Montellano, P. R., & Kerr, D. E. (1983) *J. Biol. Chem. 258*, 10558–10563.

Ortiz de Montellano, P. R., & Reich, N. O. (1986) in *Cytochrome P-450: Structure, Mechanism, and Biochemistry* (Ortiz de Montellano, P. R., Ed.) pp 273–314, Plenum Press, New York.

Ortiz de Montellano, P. R., Kunze, K. L., & Augusto, O. (1982) *J. Am. Chem. Soc. 104*, 3545–3546.

Poulos, T. L., & Howard, A. J. (1987) *Biochemistry 26*, 8165–8174.

Poulos, T. L., Perez, M., & Wagner, G. C. (1982) *J. Biol. Chem. 257*, 10427–10429.

Poulos, T. L., Finzel, B. C., Gunsalus, I. C., Wagner, G. C., & Kraut, J. (1985) *J. Biol. Chem. 260*, 16122–16130.

Poulos, T. L., Finzel, B. C., & Howard, A. J. (1986) *Biochemistry 25*, 5314–5322.

Poulos, T. L., Finzel, B. C., & Howard, A. J. (1987) *J. Mol. Biol. 195*, 687–700.

Raag, R., & Poulos, T. L. (1989a) *Biochemistry 28*, 917–922.

Raag, R., & Poulos, T. L. (1989b) *Biochemistry 28*, 7586–7592.

Ringe, D., Petsko, G. A., Kerr, D. E., & Ortiz de Montellano, P. R. (1984) *Biochemistry 23*, 2–4.

Ruf, H. H., Ahr, H., Nastainczyk, W., Ullrich, V., Mansuy, D., Battioni, J.-P., Montiel-Montoya, R., & Trautwein, A. (1984) *Biochemistry 23*, 5300–5306.

Sligar, S. G., & Murray, R. I. (1986) in *Cytochrome P-450: Structure, Mechanism, and Biochemistry* (Ortiz de Montellano, P. R., Ed.) pp 429–503, Plenum Press, New York.
Uehleke, H., Hellmer, K. H., & Tabarelli, S. (1973) *Xenobiotica 3*, 1–11.
Wagner, G. C., & Gunsalus, I. C. (1982) in *The Biological Chemistry of Iron* (Dunford, H. B., Dolphin, D., Raymond, K., & Sieker, L., Eds.) pp 405–412, Riedel, Boston.
Wolf, C. R., Mansuy, D., Nastainczyk, W., Deutschmann, G., & Ullrich, V. (1977) *Mol. Pharmacol. 13*, 698–705.

Intrinsic Fluorescence of a Truncated *Bordetella pertussis* Adenylate Cyclase Expressed in *Escherichia coli*†

Anne-Marie Gilles,‡ Hélène Munier,‡ Thierry Rose,‡ Philippe Glaser,§ Evelyne Krin,§ Antoine Danchin,*,§ Claudine Pellecuer,‡ and Octavian Bârzu*,‡

Unité de Biochimie des Régulations Cellulaires and Unité de Régulation de l'Expression Génétique, Institut Pasteur, 75724 Paris Cedex 15, France

Received March 15, 1990; Revised Manuscript Received May 11, 1990

ABSTRACT: A truncated, 432 residue long, *Bordetella pertussis* adenylate cyclase expressed in *Escherichia coli* was analyzed for intrinsic fluorescence properties. The two tryptophans (Trp69 and Trp242) of adenylate cyclase, each situated in close proximity to residues important for catalysis or binding of calmodulin (CaM), produced overlapping fluorescence emission bands upon excitation at 295 nm. CaM, alone or in association with low concentrations of urea, induced important modifications in the spectra of adenylate cyclase such as shifts of the maxima and change in the shape of the bands. From these changes and from the fluorescence spectrum of a modified form of adenylate cyclase, in which a valine residue was substituted for Trp242, it was deduced that, upon binding of CaM to the wild-type adenylate cyclase, only the environment of Trp242 was affected. The fluorescence maximum of this residue, which is more exposed to the solvent than Trp69 in the absence of CaM, is shifted by 13 nm to shorter wavelength upon interaction of protein with its activator. Trypsin cleaved adenylate cyclase into two fragments, one carrying the catalytic domain, and the second carrying the CaM-binding domain (Ladant et al., 1989). The isolated peptides conserved most of the environment around their single tryptophan residues, as in the intact adenylate cyclase, which suggests that the two domains of truncated *B. pertussis* adenylate cyclase also conserved most of their three-dimensional structure in the isolated forms.

Formation of adenosine 3′,5′-cyclic monophosphate (cAMP)[1] from ATP through the reaction catalyzed by adenylate cyclase is part of an important metabolic regulatory mechanism in living cells. While the chain of events leading to activation of adenylate cyclase, and the consequences of the increased cAMP in various prokaryotes or eukaryotes, is fairly well-known (Ullmann & Danchin, 1983; Gilman, 1984; Gancedo et al., 1985), much less is known about adenylate cyclase itself. In the absence of any structural data on the protein, it is very difficult to understand the catalytic and regulatory mechanisms governing this particular group of ATP-dependent enzymes.

Bordetella pertussis adenylate cyclase, a calmodulin (CaM) activated enzyme, is the object of intensive investigations due to its possible involvement in the virulence of this bacteria (Weiss & Hewlett, 1986). Synthesized as a large precursor of 1706 amino acid residues (Glaser et al., 1988), the protein of apparent molecular mass on SDS–PAGE of 200–215 kDa was shown to enter eukaryotic cells provoking unregulated synthesis of cAMP and ultimately cell death (Rogel et al., 1988; Gilboa-Ron et al., 1989; Hewlett et al., 1989; Masure & Storm, 1989; Bellalou et al., 1990). Tryptic digestion converted adenylate cyclase to a fully active form of 43 kDa. Further cleavage of this low molecular mass form of adenylate cyclase gives two complementary fragments corresponding to the catalytic and CaM-binding domains of protein. Isolated fragments have very little or no activity; however, upon reassociation, the CaM-dependent adenylate cyclase activity is restored to a significant level (Ladant et al., 1989). In the present paper we examined the fluorescence properties of a truncated *B. pertussis* adenylate cyclase expressed in *Escherichia coli* by taking advantage of the fact that the low molecular mass form of enzyme has two tryptophan residues, each situated in close proximity to residues important for catalysis or binding of CaM (Glaser et al., 1989).

Experimental Procedures

Chemicals. Adenine nucleotides, substrates, restriction enzymes and T_4 DNA ligase were from Boehringer Mannheim. CaM–agarose, bovine brain CaM, TPCK–trypsin, and soybean trypsin inhibitor were from Sigma. Urea (fluorimetrically pure) was a product of Schwarz/Mann. [α-^{32}P]-

† This work was supported by grants from the Centre National de la Recherche Scientifique (URA 1129), the Fondation pour la Recherche Médicale, the Ministère de la Recherche et de la Technologie (Grant 88.T.0823), and The Pasteur Weizmann Council.
* Correspondence should be addressed to these authors.
‡ Unité de Biochimie des Régulations Cellulaires.
§ Unité de Regulation de l'Expression Génétique.

[1] Abbreviations: 3′dATP, 3′-deoxyadenosine 5′-triphosphate; cAMP, adenosine 3′,5′-cyclic monophosphate; CaM, calmodulin; EGTA, [ethylenebis(oxyethylenenitrilo)]tetraacetic acid; IPTG, isopropyl β-D-thiogalactoside; TPCK, L-1-(tosylamino)-2-phenylethyl chloromethyl ketone; SDS–PAGE, sodium dodecyl sulfate–polyacrylamide gel electrophoresis.

0006-2960/90/0429-8126$02.50/0